

# Description of the submicron aerosol vertical profile in the lower troposphere by the three-layer representation

M.V. Panchenko and S.A. Terpugova

*Institute of Atmospheric Optics,  
Siberian Branch of the Russian Academy of Sciences, Tomsk*

Received July 26, 1999

It is proposed to use the notion of a three-layer aerosol vertical profile as a first approximation in the lower troposphere: the interval from 0 to  $H_1$  is the ground layer, the interval from  $H_1$  to  $H_2$  is the mixing layer, and above that is the free atmosphere. The ground layer is parametrized relative to baric formations. The height of the mixing layer was calculated on the basis of data on the total degree of heating of the lower layers. The slope of the profile in the mixing layer was estimated from its statistical correlation with the ground-level value of the scattering coefficient and the average temperature of the mixing layer.

The present paper, based on airborne nephelometer data<sup>1,2</sup> in the lower troposphere above Western Siberia, discusses the possibility of a simple parametrization of the vertical profile of the submicron particle content in the lower troposphere. As a parameter associated with the particle concentration we consider the scattering coefficient for zero relative humidity  $\sigma_d(H)$ .<sup>2</sup>

Earlier studies have shown that the main seasonal trends of the variability of  $\sigma_d(H)$  profiles are represented fairly adequately by a three-layer height distribution of the aerosol content.<sup>2,3</sup> Such a representation is depicted schematically in Fig. 1. The following altitude ranges are distinguished: 1) the ground layer with height  $H_1$ , in which significant diurnal variations of the aerosol and meteorological parameters are observed; 2) the boundary layer, or mixing layer (according to the definition of K.Ya. Kondrat'ev<sup>4,5</sup> – the zone of active turbulent exchange), in which the height  $H_2$  varies from season to season and the aerosol concentration and aerosol optical characteristics are generally assumed to be constant with height; 3) the layer of free atmosphere. Between the mixing layer and the free atmosphere, as a rule, lies a transitional zone of thickness ~200–400 m.

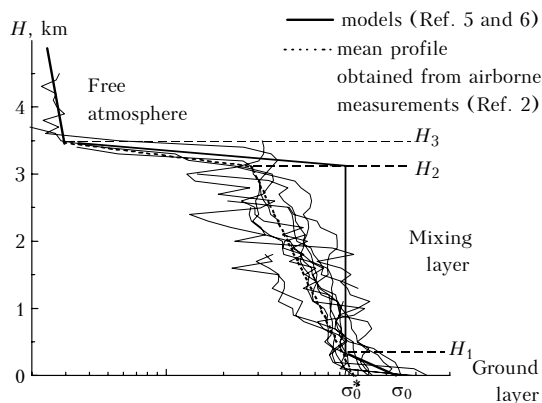


**Fig. 1.** Representation of the vertical profile of the scattering coefficient as three layers.

We consider the applicability of such an approach to discrete realizations of the aerosol profile for a specific region. All of the available measured profiles were analyzed as to the possibility of representing them as three layers.<sup>7</sup> The points  $H_1$ ,  $H_2$ , and  $H_3$  were determined from a graph of the corresponding profile as the heights at which the rate of falloff of the scattering coefficient of dry aerosol with increasing height undergoes an abrupt change. In each of the layers the profile was approximated by the formula

$$\sigma_d(H) = \sigma_d(H_{0,i}) \exp[-\alpha_i(H - H_{0,i})], \quad (1)$$

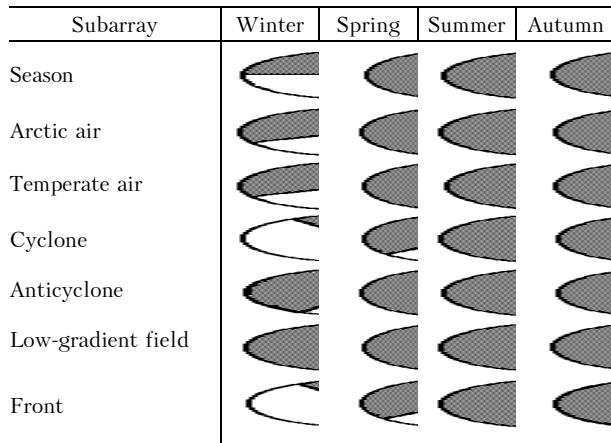
where  $H$  is the height,  $\alpha_i$  is a parameter defining the slope of the profile in the corresponding layer; and  $H_{0,i}$  is the lower boundary of the layer in question.

Table 1 lists the corresponding mean-seasonal values of the heights and the profile slope parameters  $\alpha_i$  [see formula (1)].

**Table 1.** Mean-seasonal values of the parameters of the three-layer approximation of the scattering coefficient profile

|        | $H_1$ , km | $H_2$ , km | $H_3$ , km | $\alpha_1$ | $\alpha_2$ | $\alpha_3$ | $\alpha_4$ |
|--------|------------|------------|------------|------------|------------|------------|------------|
| Winter | 0.03       | 0.28       | 0.38       | 0.35       | 7.5        | 2.6        | 0.71       |
| Spring | 0.04       | 1.26       | 1.58       | 4.0        | 0.29       | 3.0        | 0.4        |
| Summer | 0.06       | 1.94       | 2.2        | 1.9        | 0.19       | 5.2        | 0.44       |
| Autumn | 0.08       | 1.25       | 1.55       | 3.1        | 0.34       | 4.5        | 0.34       |

Figure 2 shows pie charts which show what percent of the realizations of a given data set is satisfactorily described by the three-layer representation. It can be seen from the figure that representing the vertical profile as three layers is most valid in summer; in winter it is applicable only for a limited number of situations. In spring and autumn this representation is realized mainly under stable weather conditions in nearly stagnant air masses, i.e., the three-layer model affords a good description of the aerosol vertical profile for situations in which the process of formation of the profile is sufficiently extended. Under other conditions the profile has a more complicated multilayer structure.



**Fig. 2.** Applicability of the three-layer model to description of vertical profiles of the scattering coefficient in different synoptic situations.

Let us now consider the parametrization of the aerosol profile in each layer in more detail.

The ground layer of the atmosphere at a height of 100 m is the most variable. The largest variations of both the meteorological parameters and the aerosol particle concentration are seen in it, and the influence of the underlying surface, season, time of day, wind speed and direction, etc. is greatest in it. In existing models<sup>4-6</sup> for the ground layer the aerosol concentration decreases abruptly with height. However, the measurement data show that this is not always the case. The presence of a temperature inversion may serve as a quite reliable criterion of the existence of a ground layer in the vertical aerosol profile, but these data are not always available; therefore, we made an attempt to estimate the parameters of the aerosol profile in the ground layer from synoptic indicators.

Table 2 presents data for different seasons on the percentage of realizations in different air masses and baric formations in which the presence of an aerosol ground layer is observed. A pronounced aerosol ground layer is almost always observed in summer and autumn in arctic air masses while in temperate air masses only in regions of increased pressure. In temperate air masses in autumn and spring the parametrization cannot be realized due to poor statistics of the data.

No significant dependence of the existence of the ground layer on the time of day was observed in our data.

In the mixing layer the aerosol content is often assumed to be constant with height.<sup>5,6</sup> But, as an analysis of a large body of experimental data shows (these data are depicted in Fig. 1 by thin lines) this representation is valid only as a first approximation since under conditions, in which the main aerosol sources are located at ground level, a flat aerosol profile with height would require practically instantaneous mixing.

Different approaches to estimation of the mixing layer height can be found in literature.<sup>5,9-11</sup> However, estimating this height through the activity of turbulent exchange (which from the point of view of the main mechanism is absolutely valid), a number of problems arise since processes of turbulent exchange along the vertical are strongly influenced by the temperature profile and the state of the underlying surface, and also gradual day-to-day heating (or cooling) of the entire lower troposphere. Aerosol processes have much more inertia, and the height  $H_2$  is due to comparatively prolonged mixing of particles along the vertical,<sup>11</sup> taking place over the lifetime of the given air mass.

**Table 2.** The portion of profiles (%) modeling of which requires to take into account the ground aerosol layer

| Spring              |     |         |     |                     |     |         |    |
|---------------------|-----|---------|-----|---------------------|-----|---------|----|
| Arctic air – 44     |     |         |     | Temperate air – 26  |     |         |    |
| Cyclone             | –   | day     | 37  | Cyclone             | 33  | day     | 14 |
| Anticyclone         | 25  | evening | 72  | Anticyclone         | 66  | evening | 67 |
| Low-gradient field  | –   | night   | 33  | Low-gradient field  | 0   | night   | 40 |
| Ridge               | 50  | morning | –   | Ridge               | –   | morning | –  |
| Low-pressure trough | –   |         |     | Low-pressure trough | –   |         |    |
| Summer              |     |         |     |                     |     |         |    |
| Arctic air – 75     |     |         |     | Temperate air – 50  |     |         |    |
| Cyclone             | 85  | day     | 67  | Cyclone             | 25  | day     | 46 |
| Anticyclone         | 75  | evening | 50  | Anticyclone         | 100 | evening | 50 |
| Low-gradient field  | 100 | night   | 92  | Low-gradient field  | 100 | night   | 52 |
| Ridge               | 100 | morning | 100 | Ridge               | 67  | morning | –  |
| Low-pressure trough | –   |         |     | Low-pressure trough | 33  |         |    |
| Autumn              |     |         |     |                     |     |         |    |
| Arctic air – 63     |     |         |     | Temperate air – 57  |     |         |    |
| Cyclone             | 60  | day     | 57  | Cyclone             | 40  | day     | 50 |
| Anticyclone         | 63  | evening | 50  | Anticyclone         | 67  | evening | 52 |
| Low-gradient field  | 50  | night   | 77  | Low-gradient field  | –   | night   | 67 |
| Ridge               | –   | morning | –   | Ridge               | 80  | morning | –  |
| Low-pressure trough | 34  |         |     | Low-pressure trough | –   |         |    |

For a definite height of the mixing layer for each profile we calculated the mean temperature  $\bar{T}_i$  of layers of different height. Figure 3 shows two scatter plots of the height of the mixing layer and the mean temperature of the layer from 0 to 3 km. It is evident from the figure that the relation between  $H_2$  and  $\bar{T}_3$  is nonlinear, and when the data are replotted on a logarithmic scale in height it becomes linear. Table 3 lists the correlation coefficients between the mixing layer height and the mean temperature of layers of different height.

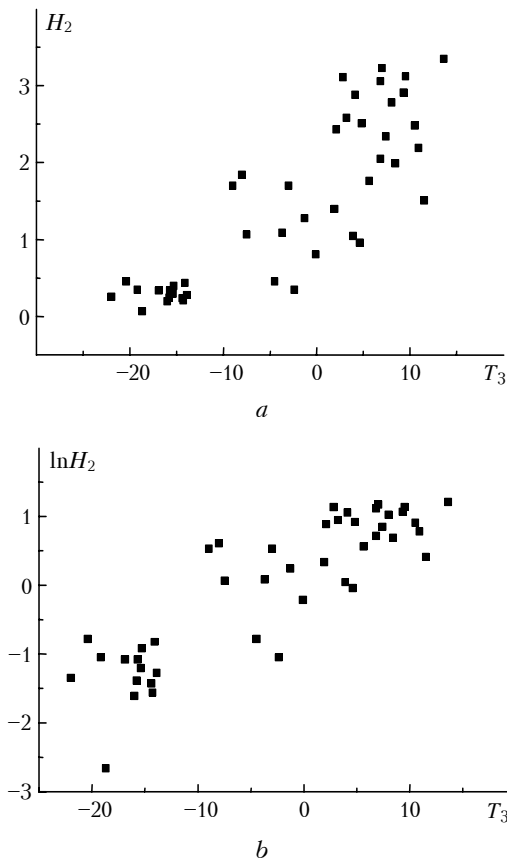


**Fig. 3.** Scatter plots of the height of the mixing layer and the mean temperature of the 0–3 km layer: (a) linear scale in height; (b) logarithmic scale.

From this we conclude that the relation between the height of the mixing layer  $H_2$  and the temperature  $\bar{T}_i$  is adequately expressed in the form

$$\ln(H_2) = A_i \bar{T}_i + B_i. \tag{2}$$

Figure 4 plots the dependence of the coefficients  $A$  and  $B$  on the height of the layer, over which the temperature has been averaged.

We see that the dependences are nearly linear, which gives a basis to estimate these coefficients from the following regression equations:

$$A = -0.514 + 0.173 H; \tag{3}$$

$$B = 0.042 + 0.0094 H.$$

**Table 3.** Correlation coefficients between the mixing layer height and mean temperature of the atmospheric layers of different height

| $H$ , km | $\rho_{H_2, \bar{T}_i}$ | $\rho_{\ln H_2, \bar{T}_i}$ |
|----------|-------------------------|-----------------------------|
| 0.5      | 0.56                    | 0.76                        |
| 1        | 0.61                    | 0.80                        |
| 1.5      | 0.65                    | 0.80                        |
| 2        | 0.67                    | 0.81                        |
| 2.5      | 0.70                    | 0.82                        |
| 3        | 0.72                    | 0.82                        |
| 3.5      | 0.73                    | 0.83                        |
| 4        | 0.5                     | 0.87                        |
| 4.5      | 0.74                    | 0.84                        |
| 5        | 0.73                    | 0.84                        |

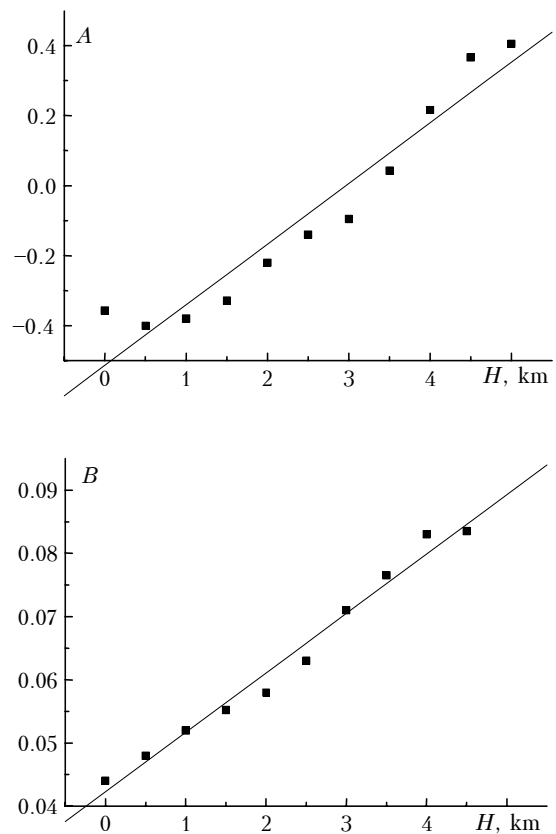


**Fig. 4.** Coefficients of the regression formula to reconstruct the height of the mixing layer.

Consequently, to estimate the height  $H_2$ , we can use the following combined dependence:

$$H_2 = 0.6 \exp [(0.04 + 0.01 \tilde{H}) T_{\tilde{H}} + 0.2 \tilde{H}], \tag{4}$$

where  $T_{\tilde{H}}$  is the mean temperature of the layer, °C, lying at the height  $\tilde{H}$ , km.

The main factors determining the slope of the profile in the mixing layer can be the following:

- 1) the intensity of the ground-level aerosol sources;
- 2) the rate of aerosol transport in the vertical direction.

As a parameter characterizing the intensity of the ground-level aerosol sources, we may consider the ground-level value of the scattering coefficient  $\sigma_0$ . (In our earlier estimate of the parameters of the mixing layer<sup>8</sup> we did not consider it. In the case where it shows up distinctly in the experimental data, to retrieve  $\sigma(H)$  we used the value  $\sigma_0^*$ , defined by extrapolating the profile in the mixing layer down to ground level).

It is well known that the velocities of ordered vertical movements in the atmosphere are determined by the temperature gradient.<sup>12,13</sup> And of course, in the first phase of our work, we attempted to relate the profile slope parameter in the mixing layer  $\alpha_2$  to the mean temperature gradient in this layer. The corresponding scatter plot is shown in Fig. 5 where the value of the correlation coefficient is also indicated. No direct relationship between the parameters is seen. This is completely understandable since the process of aerosol mixing along the vertical has a much longer delay time than variations in temperature stratification. Therefore, it is much more logical to link the slope of the profile with the mean degree of heating of the lower layers of the atmosphere than with the temperature gradient (by degree of heating we mean the mean temperature of the layer extending from the underlying surface to some height  $H$ ).

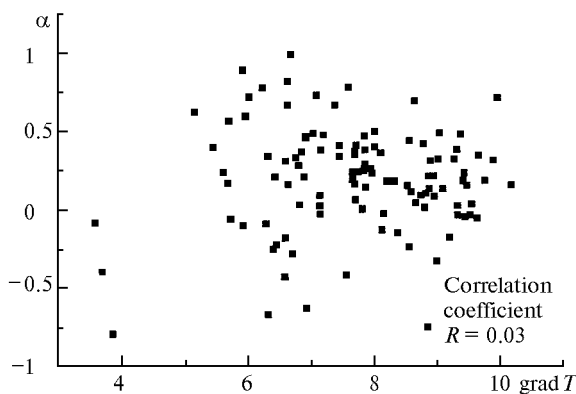


Fig. 5. Correlation diagram between the coefficient of the profile slope in the mixing layer and mean temperature gradient.

To retrieve the profile, we used the ground-level value of the scattering coefficient and the mean temperature of the 0–3 km layer  $\bar{T}_3$ . Table 4 lists total and partial correlation coefficients between the

indicated parameters for different seasons and the entire data set.

Two ways of estimating the profile slope are now possible:

- 1) from the single parameter  $\sigma_0$ . In this case we constructed the following regression formula:

$$\alpha_2 = 0.89 + 0.24 \ln \sigma_0; \tag{5}$$

- 2) from the two parameters  $\sigma_0$  and  $\bar{T}_3$  (here we constructed a two-parameter linear regression):

$$\alpha_2 = 0.26 + 0.1 \ln \sigma_0 + 0.02 \bar{T}_3, \tag{6}$$

where  $\sigma_0$  is in  $\text{km}^{-1}$  and temperature is in  $^\circ\text{C}$ .

Table 4. Total and partial correlation coefficients of the slope of the profile in the mixing layer with the logarithm of the ground-level value of the scattering coefficient and the mean temperature of the 0–3 km layer

| Correlation coefficient                 | Spring | Summer | Autumn | All seasons |
|---|--------|--------|--------|-------------|
| $\rho_{\alpha, \ln \sigma_0}$           | 0.37   | 0.55   | 0.51   | 0.50        |
| $\rho_{\alpha, \bar{T}}$                | 0.32   | 0.45   | 0.38   | 0.41        |
| $\rho_{\alpha, \ln \sigma_0   \bar{T}}$ | 0.52   | 0.65   | 0.55   | 0.57        |
| $\rho_{\alpha, \bar{T}   \ln \sigma_0}$ | 0.15   | 0.20   | 0.16   | 0.18        |

Table 5. Standard deviation of the profile slope parameter in the mixing layer, determined using regression formulas (5) and (6)

| Standard deviation                       | Spring | Summer | Autumn |
|--|--------|--------|--------|
| Initial data set                         | 0.37   | 0.34   | 0.37   |
| Determined from $\sigma_0$               | 0.25   | 0.18   | 0.24   |
| Determined from $\sigma_0$ and $\bar{T}$ | 0.20   | 0.14   | 0.20   |

Table 5 lists the standard deviation of the parameter  $\alpha_2$  determined using regression formulas (5) and (6).

For the free atmosphere we took the mean-seasonal values of the profile parameters since it is clear that in this layer the aerosol content is already much less correlated with the ground-level sources at the observation point and has a regional character. Consequently, retrieval of the profile using only  $\sigma_0$  is not expedient.

Figure 6 plots the rms error

$$\varepsilon(H) = \sqrt{\frac{1}{N-1} \sum_{i=1}^N [\sigma_{\text{retr}}(H) - \sigma_{\text{meas},i}(H)]^2}$$

retrieval of the "dry" aerosol scattering coefficient profile in the mixing layer for different seasons taking into account one  $\sigma_0$  or both ( $\sigma_0$  and  $\bar{T}_3$ ) parameters.

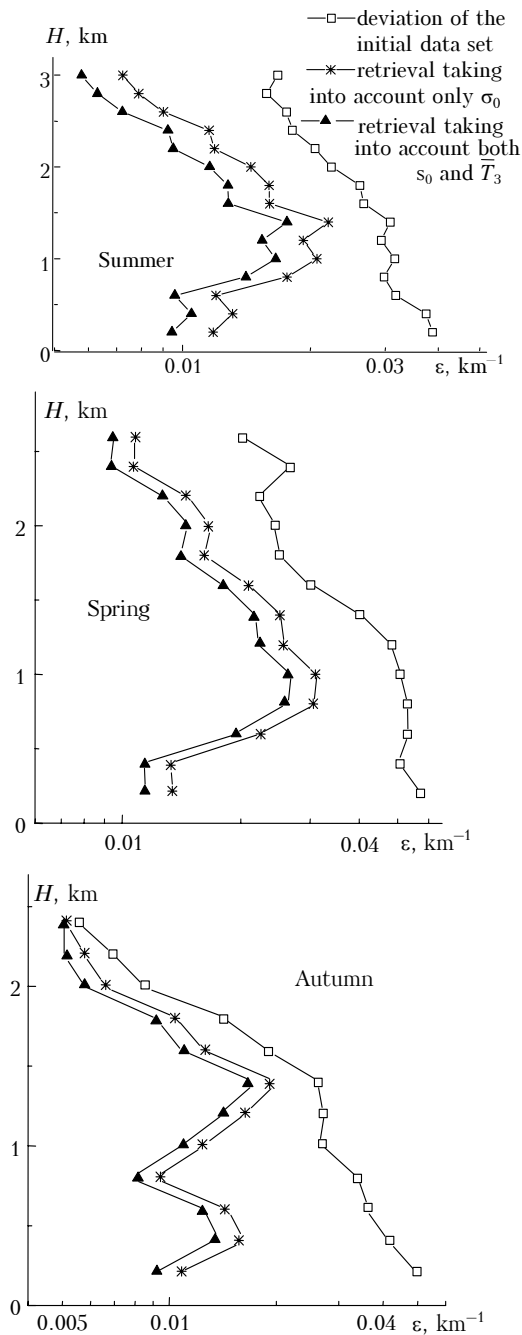


Fig. 6. RMS error of retrieval of the aerosol scattering coefficient profile in the mixing layer for different seasons.

From Fig. 6 it can be seen that taking the ground-level value of the scattering coefficient and the mean temperature of the lower layers into account makes it possible to decrease the rms error of retrieval of the vertical aerosol profile in the mixing layer by more than a factor of two in comparison with the standard deviation of the initial data set for seasons of the year when the main aerosol sources are located at ground level.

### Acknowledgments

This work was carried out with financial support from the Russian Foundation for Basic Research (Grant No. 95-05-14195).

### References

1. M.V. Panchenko and S.A. Terpugova, *Atmos. Oceanic Opt.* **7**, No. 8, 546-551 (1994).
2. M.V. Panchenko and S.A. Terpugova, *Atmos. Oceanic Opt.* **7**, No. 8, 552-557 (1994).
3. Yu.P. Dyabin, M.V. Tantashev, S.O. Murumyants, and V.D. Marusyak, *Izv. Akad. Nauk SSSR, Ser. Fiz. Atmos. Okeana* **13**, No. 11, 1205-1211 (1977).
4. K.Ya. Kondrat'ev, ed., *Aerosol and Climate* (Gidrometeoizdat, Leningrad, 1991), 542 pp.
5. K.Ya. Kondrat'ev, N.I. Moskalenko, and D.V. Pozdnyakov, *Atmospheric Aerosol* (Gidrometeoizdat, Leningrad, 1983), 224 pp.
6. V.E. Zuev and G.M. Krekov, *Optical Models of the Atmosphere* (Gidrometeoizdat, Leningrad, 1986), 256 pp.
7. S.A. Terpugova and M.V. Panchenko, in: *Abstracts of Reports at the Second Inter-Republic Symposium on Optics of the Atmosphere and Ocean*, Tomsk, (1995), p. 78.
8. S.A. Terpugova and M.V. Panchenko, in: *Abstracts of Reports at the Second Inter-Republic Symposium on Optics of the Atmosphere and Ocean*, Tomsk, (1996), p. 83.
9. B.D. Belan, *Atmos. Oceanic Opt.* **7**, No. 8, 558-562 (1994).
10. N.L. Byzova, E.K. Garger, and V.N. Ivanov, *Experimental Studies of Atmospheric Diffusion and Calculations of Spreading of Pollutants* (Gidrometeoizdat, Leningrad, 1991), 280 pp.
11. I.N. Kuznetsova, *Proceedings of the Hydrometeorological Center of the USSR*, No. 289, 99-103 (1989).
12. D.L. Laikhtman, ed., *Dynamic Meteorology* (Gidrometeoizdat, Leningrad, 1976), 608 pp.
13. L.T. Matveev, *Course in General Meteorology. Atmospheric Physics* (Gidrometeoizdat, Leningrad, 1984), 752 pp.